

# J80-133 Shear Modulus of New Sandwich Cores Made of Superplastic Sheet

C.E.S. Ueng,\* E. E. Underwood†  
Georgia Institute of Technology, Atlanta, Ga.

and

T. L. Liu‡  
Evans Products Co., Chamblee, Ga.

### Introduction

THE conventional aluminum foil, hexagonal cell core has dominated the sandwich construction for structural applications. In view of the fact that only one basic cell shape is generally available, it seriously limits the flexibility and optimization parameters desired for a wide range of load environments. In order to circumvent this and other drawbacks, a new method of producing sandwich cores of a wide variety of shapes, using low-load superplastic sheet forming, was adopted at the Georgia Institute of Technology.<sup>1</sup> Several core configurations, consisting of projections with different shapes and symmetries in simple locational arrays, are produced and tested. Comparisons with predictions from optimization studies are thus possible, leading themselves to an interactive feedback between analysis and experiment and, ultimately, to optimized core designs. Previous reports have been published on the maximization of the shear modulus of the core<sup>2-4</sup> and on the analysis of least-weight core configurations.<sup>5,6</sup> This Note shows how these procedures supply solutions to a wide range of core design problems of interest to those seeking greater structural efficiency.

### Shear Modulus

As in many literature references,<sup>7,8</sup> the core in a sandwich panel is essentially assumed to resist the transverse shear forces in a way similar to the function of the web portion in an I-beam. Therefore, the determination of the shear modulus of the core is one of the most important and significant tasks. Due to the complexity of the core geometry, exact solution of the shear modulus seems to be a formidable task to carry out. In view of this, energy principles are used for obtaining approximate solutions which turn out to be the lower and upper bounds. From these bounds, one can assess the degree of accuracy provided by the approximate solution. In this Note, a core configuration consisting of truncated, hollow, hexagonal pyramidal projections positioned in a simple square array is considered. Figure 1 shows a unit projection of a six-sided truncated pyramid in the core, as well as a typical cross section of the projection.

In order to make the analysis more tractable, the following assumptions are adopted: 1) the complete core structure is made up of identical projections where the number of projections in a given panel is large enough that any local and/or boundary effects can be ignored; 2) the core is well manufactured so that all projections can be assumed to be identical; 3) the effect of the small radius at the corners of a core projection due to manufacturing is negligible; 4) the wall

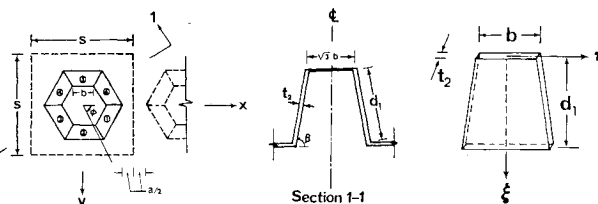


Fig. 1 Unit projection of a six-sided truncated pyramid in the core.

thickness at different locations in the projections is the same, and is small in comparison with other dimensions; 5) buckling or warping of the inclined walls in the core projections is excluded from consideration; and 6) the core is assumed to behave in a linearly elastic fashion.

Following Kelsey et al.<sup>9</sup> and Argyris,<sup>10</sup> we denote the direction of the applied force by subscript 1 and the direction normal to it (in the horizontal  $x$ - $y$  plane) by subscript 2. Due to the anisotropic nature of the core, the direction of the resultant shear displacement  $\Delta$  does not usually coincide with the direction of the applied shear force. We can, however, resolve  $\Delta$  into two components along directions 1 and 2. The shear stresses and shear strains along these two directions can be expressed as

$$\begin{bmatrix} \gamma_1 \\ \gamma_2 \end{bmatrix} = \begin{bmatrix} f_{11} & f_{12} \\ f_{21} & f_{22} \end{bmatrix} \begin{bmatrix} \tau_1 \\ \tau_2 \end{bmatrix} \quad (1)$$

where  $f_{ij}$  is the flexibility matrix. If, on the other hand, the core is constrained in such a way that the displacement occurs along a given direction, say 1, then it will not only require a force in direction 1 but also a force along the perpendicular direction, i.e., direction 2. The ratios of these individual forces to the displacements represent the stiffness property of the core. The shear property of the core can, therefore, also be expressed as

$$\begin{bmatrix} \tau_1 \\ \tau_2 \end{bmatrix} = \begin{bmatrix} k_{11} & k_{12} \\ k_{21} & k_{22} \end{bmatrix} \begin{bmatrix} \gamma_1 \\ \gamma_2 \end{bmatrix} \quad (2)$$

where  $k_{ij}$  is the stiffness matrix. It is well known that the flexibility matrix  $[f]$  can also be calculated from  $[k]$  by the following relation, i.e.,

$$[f] = [k]^{-1} \quad (3)$$

Note that the results on  $[f]$ , as computed from Eqs. (1) and (3), should be the same if the exact stress (or strain) distribution due to the applied shear (or displacement) is known. From the shape of the sandwich core, it is quite obvious that an exact stress field inside the core structure is certainly too difficult to determine. Furthermore, the procedure of isolating the unit core projection from the remaining part would not even be correct for an exact analysis.

In the following, two energy principles are employed to obtain the approximate solutions. These are: 1) the flexibility matrix is determined by the unit load method where the stress distribution in the core due to applied shear stresses  $\tau_1$  and  $\tau_2$  is assumed, and 2) the stiffness matrix is determined by the unit displacement method where a simple form is assumed for the strain distribution in the core due to imposed shear strains  $\gamma_1$  and  $\gamma_2$ . As shown by Argyris,<sup>10</sup> these two methods yield upper and lower bounds to the flexibility, i.e., the flexibility of the core is overestimated by the unit load method and underestimated by the unit displacement method.

### A. Upper Bounds

The determination of an upper bound for the shear modulus is accomplished by the unit displacement method,

Presented as Paper 79-0754 at the AIAA/ASME/ASCE/AHS 20th Structures, Structural Dynamics and Materials Conference, St. Louis, Mo., April 4-6, 1979; submitted May 14, 1979; revision received Oct. 15, 1979. Copyright © American Institute of Aeronautics and Astronautics, Inc., 1979. All rights reserved.

Index categories: Structural Composite Materials; Materials, Properties of; Structural Materials.

\*Professor, School of Engineering Science and Mechanics.

†Professor of Metallurgy.

‡Structural Engineer.

except that our unit "displacements" in this problem are the applied unit shear strains. Here, the exact stress distribution due to a unit overall shear strain is unknown. The approximate results for the stiffnesses are obtained by calculating the stresses as due to strains kinematically equivalent to the imposed unit strain. We assume that the faces of the projections remain plane during shear displacement and that the shear strain in each inclined wall is constant over the entire wall. Applying the principle of virtual work and taking account only of the shear stress in the plane of each of the six inclined walls in a unit projection, the stiffness  $k_{ij}$  can be written as:

$$k_{ij} = \left\{ \sum_{n=1}^6 (\gamma_{ni} \gamma_{nj}) G t_2 d_1 (b + d_1 \cos \beta \cot 60^\circ) \right\} / S^2 d_1 \sin \beta \quad (i, j = 1, 2) \quad (4)$$

where  $b$ ,  $t_2$ ,  $d_1$ ,  $\beta$ , and  $S$  are parameters describing the dimensions of the core (see Fig. 1);  $G$  is the shear modulus of the core material in bulk; and  $\gamma_{ni}$  is the shear strain in plane  $n$  due to unit shear strain  $\gamma_i$  on the core as a whole. Considering that  $\gamma_1 = 1$  and  $\gamma_2 = 1$ , respectively, we can find  $\gamma_{ni}$  and  $\gamma_{nj}$ . Substituting these into Eq. (4), we obtain the effective shear modulus of the core according to the unit displacement (unit shear strains here) method, i.e.,

$$G_D = [3 G t_2 (b + d_1 \cos \beta \cot 60^\circ) \sin \beta] / S^2 \quad (5)$$

where

$$S = 2(b + d_1 \cos \beta \csc 60^\circ) + a \quad (6)$$

### B. Lower Bounds

The determination of a lower bound is similarly accomplished by the unit load method, except that our unit "loads" are the unit shear stresses  $\tau_1$  and  $\tau_2$  acting on the core as a whole. The resulting shear flows developed in the inclined walls of a projection due to the unit shear stresses  $\tau_1$  and  $\tau_2$  can be computed from the conditions of equilibrium within the core. The flexibility  $f_{ij}$  can be expressed in the following form

$$f_{ij} = \left\{ \int_0^{d_1} \int_{-(b/2 + \xi \cos \beta \cot 60^\circ)}^{b/2 + \xi \cos \beta \cot 60^\circ} \left[ \sum_{n=1}^6 \frac{q_{ni} q_{nj}}{t_2 G} \right] d\eta d\xi \right\} + S^2 d_1 \sin \beta \quad (i, j = 1, 2) \quad (7)$$

where  $\xi$ - $\eta$  is a local coordinate system with its origin at the center of the top edge of each inclined panel as shown in Fig. 1.  $q_{ni}$  is the shear flow in the inclined panel  $n$  at level  $\xi \sin \beta$  from the top area of the core due to a unit shear stress  $\tau_i$  acting on the core. By the equilibrium requirement, the shear flows can then be computed. Upon substituting these into Eq. (7), we have the lower bound of the shear modulus,

$$G_L = \begin{cases} \frac{54 G t_2 d_1 \sin 2\beta}{\sqrt{3} S^2 \ln \left( 1 + \frac{2\sqrt{3}}{3} \frac{d_1}{b} \cos \beta \right) (21 - \cos^2 \phi)} & \text{if } 0 < \beta < \frac{\pi}{2} \\ \frac{54 G t_2 b}{S^2 (21 - \cos^2 \phi)} & \text{if } \beta = \frac{\pi}{2} \end{cases} \quad (8)$$

### Comparison of Analytical and Experimental Results

Upper and lower bounds from dimensionless parameters for  $G_D$  and  $G_L$  are plotted in Figs. 2 and 3. Figure 2 refers to the case for  $\phi = 0$  deg, while Fig. 3 represents the case for  $\phi = 90$  deg, where  $\phi$  is the angle measured from the  $x$  direc-

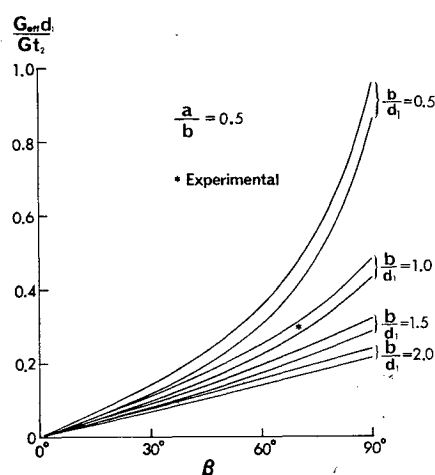


Fig. 2 Upper and lower bounds of nondimensional shear modulus vs the inclination angle  $\beta$ ,  $\phi = 0$  deg.

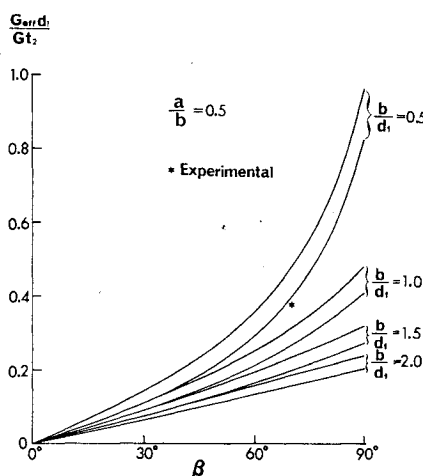


Fig. 3 Upper and lower bounds of nondimensional shear modulus vs the inclination angle  $\beta$ ,  $\phi = 90$  deg.

tion. These two diagrams indicate that the upper and lower bounds of the nondimensionalized shear modulus are clearly distinguishable according to the value assigned to the ratio  $b/d_1$  in the computational work. For small  $\beta$ , those two bounds almost coincide with each other. As  $\beta$  increases, however, the divergence between these two bounds also increases to about  $\pm 10\%$  of the mean.

The two starred points shown in Figs. 2 and 3 for  $b/d_1 = 1.0$  represent typical experimental data obtained from core shear tests. The results appear to confirm the analytical results quite well.

The results obtained here for the shear modulus of superplastically formed sandwich cores provide an attractive engineering solution to the analytical problem. In addition, the methodology can be used to supply engineering solutions to a class of problems which concern greater structural efficiency. The superplastic forming method provides an inexpensive way to achieve configurational optimization, as well as substantial cost and weight savings.

Other important tasks related to the topic being reported here, such as on the theory and practice of superplastic forming, furnace construction, experimental techniques, etc., will be reported in other appropriate scientific publications.

### Acknowledgment

This research was supported by a grant from the National Science Foundation, ENG 75-17968, with C. A. Babendreier, Program Director.

## References

- <sup>1</sup>Underwood, E. E., Gomez, A., and Ueng, C.E.S., "Design and Fabrication of New Core Configurations for Sandwich Panels," *Proceedings, IVth Inter-American Conference on Materials Technology*, Caracas, Venezuela, June-July 1975, p. 531.
- <sup>2</sup>Ueng, C.E.S. and Liu, T. L., "Optimization of a New Lightweight Sandwich Core," *Proceedings, International Conference on Lightweight Shell and Space Structures for Normal and Seismic Zones*, Alma-Ata, USSR, Vol. 2, Sept. 1977, pp. 375-383.
- <sup>3</sup>Ueng, C.E.S., "Superplastically Formed New Sandwich Cores," *Transportation Engineering Journal, ASCE*, July 1978, pp. 437-447.
- <sup>4</sup>Ueng, C.E.S., Underwood, E. E., and Liu, T. L., "Shear Modulus of Superplastically Formed Sandwich Cores," *Proceedings of Symposium on Future Trends in Computerized Structural Analysis and Synthesis*, Pergamon Press, edited by A. K. Noor and H. G. McComb, Jr., eds., Oct.-Nov. 1978, Washington, D.C., pp. 393-397; also *International Journal of Computers and Structures*, Vol. 10, Nos. 1 and 2, 1979, pp. 393-397.
- <sup>5</sup>Ueng, C.E.S. and Liu, T. L., "Least-Weight of Superplastically Formed Cores," *Proceedings, Second ASCE Engineering Mechanics Specialty Conference*, North Carolina State University, Raleigh, N.C., May 1977, pp. 440-443.
- <sup>6</sup>Ueng, C.E.S. and Liu, T. L., "Least-Weight Analysis of a New Sandwich Core," *Proceedings, 14th Annual Meeting of the Society of Engineering Science*, Nov. 1977, Lehigh University, Bethlehem, Pa., pp. 273-283.
- <sup>7</sup>Plantema, F. J., *Sandwich Construction*, John Wiley and Sons, New York, 1966.
- <sup>8</sup>Allen, H. G., *Analysis and Design of Structural Sandwich Panels*, Pergamon Press, New York, 1969.
- <sup>9</sup>Kelsey, S., Gellately, R. A., and Clark, B. W., "The Shear Modulus of Foil Honeycomb Core," *Aircraft Engineering*, Vol. 30, Oct. 1958, pp. 294-302.
- <sup>10</sup>Argyris, J. H., "Energy Theorems and Structural Analysis," *Aircraft Engineering*, Vol. 26, Oct.-Nov. 1954; Vol. 27, Feb., March, April, and May 1955; see also J. H. Argyris, *Energy Theorems and Structural Analysis*, Butterworth Scientific Publications, London, 1960.

## Radiative Transfer of Energy in a Cylindrical Enclosure with Heat Generation

James Higenyi\* and Yildiz Bayazitoglu†  
Rice University, Houston, Tex.

## Nomenclature

$B$	= emissive power, $\sigma_s T^4$
$Q$	= radiative heat flux
$\ell$	= direction cosine
$S$	= heat source per unit volume
$T$	= temperature
$U$	= dimensionless heat generation rate per unit volume, nondimensionalized by $\alpha\psi^*$
$\alpha$	= volumetric absorption coefficient
$\epsilon$	= emissivity of the medium
$\epsilon_w$	= emissivity of the boundaries
$\lambda$	= $\sigma/(\alpha + \sigma)$

Received July 17, 1979; revision received Oct. 22, 1979. Copyright © American Institute of Aeronautics and Astronautics, Inc., 1979. All rights reserved.

Index categories: Radiation and Radiative Heat Transfer; Combustor Designs.

\*Graduate Student, Mechanical Engineering and Materials Science Dept.

†Assistant Professor, Mechanical Engineering and Materials Science Dept. Member AIAA.

$\sigma$	= volumetric scattering coefficient
$\tau$	= $(\alpha + \sigma)r$
$\sigma_s$	= Stefan-Boltzmann constant
$\Phi$	= dimensionless emissive power, nondimensionalized by $\pi\psi^*$
$\psi$	= dimensionless intensity of radiation, nondimensionalized by $\psi$
$\psi^*$	= reference intensity of radiation
$\Omega$	= solid angle, $4\pi$

## Subscripts

$w$	= wall
$1$	= boundary
$2$	= outer boundary
$r, \theta, z$	= directions in the cylindrical coordinate system

## Introduction

To overcome the inaccuracy of the  $P_1$  approximation of the spherical harmonics method in optically thin regions, various modifications and improvements have been introduced. Olfe<sup>1</sup> obtained good results by analyzing the surface emissive power contribution exactly while utilizing  $P_1$  approximation for the gas emission contribution. Modest and Stevens<sup>2</sup> used  $P_1$  approximation and exact treatment to obtain geometric factors which improve the results. Chou and Tien<sup>3</sup> approached the problem by approximating the moments of intensity by their mean values and dividing the radiation field into solid angle subregions which accounts for the curvature effects and give better results. Yuen and Tien<sup>4</sup> obtained quite accurate results through their analysis by subdividing the concentric cylindrical enclosure into many cylindrical subsections. However, the analysis may become complex if the modifications are extended to multidimensional problems. The higher order approximations of the spherical harmonics method would retain the differential nature for multidimensional problems and may result in more accurate solutions than  $P_1$  approximations. In plane and spherical symmetric geometries, the differential approximations as high as  $P_{20}$  have been studied by Schmidt and Gelbard<sup>5</sup> and Federighi.<sup>6</sup> In cylindrical geometry  $P_3$  is the highest order approximation that has been recently analyzed by Bayazitoglu and Higenyi<sup>7</sup> for the radiative equilibrium problems of a nonscattering medium. In the present work, the higher order differential approximations, the  $P_1$ ,  $P_3$ , and  $P_5$  approximations of the spherical harmonics method, are used to study the radiative transfer in cylindrical symmetry systems.

## Analysis

The intensity of radiation  $\psi$  is expanded in a series of normalized spherical harmonics. This expansion is expressed in terms of the moments of intensity. The  $P_n$  approximation follows when one terminates the series after certain number of terms. For the cylindrical symmetry problems (one-dimensional), the  $P_3$  approximation will result in the following intensity of radiation profile

$$\begin{aligned} \pi\psi(r, \beta, \phi) = & \frac{1}{4}\psi_0 + \frac{3}{4}\psi_r \sin\beta \cos\phi + \frac{3}{8}(3\psi_{rr} - \psi_0) \\ & \times \sin^2\beta \cos 2\phi + \frac{3}{8}(5\psi_{rrr} - 3\psi_r) \sin^3\beta \cos 3\phi \\ & + 9/32(35\psi_{rrrr} - 30\psi_{rr} + 3\psi_0) \sin^4\beta \cos 4\phi \\ & + 11/32(63\psi_{rrrrr} - 70\psi_{rrr} + 15\psi_r) \sin^5\beta \cos 5\phi \end{aligned} \quad (1)$$

and the coordinate system is shown in Fig. 1. The  $P_1$  and  $P_3$  approximations correspond to the first two terms and the first seven terms of Eq. (1), respectively. The moments used in Eq. (1) are called the zeroth, first, second, and so on.